

See discussions, stats, and author profiles for this publication at: <https://www.researchgate.net/publication/51070416>

Low- and High-Frequency Raman Investigations on Caffeine: Polymorphism, Disorder and Phase Transformation

ARTICLE in THE JOURNAL OF PHYSICAL CHEMISTRY B · MAY 2011

Impact Factor: 3.3 · DOI: 10.1021/jp112074w · Source: PubMed

CITATIONS

20

READS

80

6 AUTHORS, INCLUDING:



[Alain Hédoux](#)

Université des Sciences et Technologies de L...

94 PUBLICATIONS 1,243 CITATIONS

[SEE PROFILE](#)



[Yannick Guinet](#)

Université des Sciences et Technologies de L...

86 PUBLICATIONS 1,178 CITATIONS

[SEE PROFILE](#)



[Marc Descamps](#)

Université des Sciences et Technologies de L...

65 PUBLICATIONS 1,112 CITATIONS

[SEE PROFILE](#)

Low- and High-Frequency Raman Investigations on Caffeine: Polymorphism, Disorder and Phase Transformation

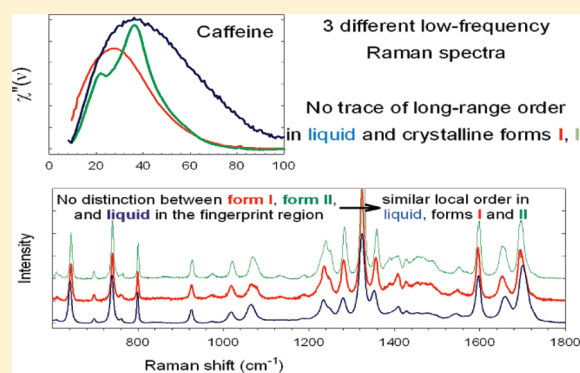
Alain Hédoux,* Anne-Amandine Decroix, Yannick Guinet, Laurent Paccou, Patrick Derollez, and Marc Descamps

Université Lille Nord de France, F-59000 Lille, France

USTL, UMET, F-59650 Villeneuve d'Ascq, France

CNRS, UMR 8207, F-59650 Villeneuve d'Ascq, France

ABSTRACT: Raman investigations are carried out both in crystalline forms of caffeine and during the isothermal transformation of the orientationally disordered form I into the stable form II at 363 K. The time dependence of the Raman spectrum exhibits no significant change in the intramolecular regime (above 100 cm^{-1}), resembling the spectrum of the liquid state. By contrast, significant changes are observed below 100 cm^{-1} , and the low-frequency spectra of forms I and II are observed to be different from that of the liquid. The temperature dependence of the $5\text{--}600\text{ cm}^{-1}$ spectrum gives information on the static disorder through the analysis of collective motions, while information on dynamic disorder are obtained from the study of the 555 cm^{-1} band corresponding to internal vibrations in the pyrimidine ring. This analysis indubitably reveals that form II is also orientationally disordered with a local molecular arrangement that mimics that in form I and the liquid state. The comparison of the low-frequency spectra recorded in theophylline and form II of caffeine allows one to describe the stable form of caffeine from the packing arrangement of anhydrous theophylline with the consideration of reorientational molecular disorder.



I. INTRODUCTION

Caffeine ($\text{C}_8\text{H}_{10}\text{N}_4\text{O}_2$) is a well-known agrochemical and therapeutic agent. Anhydrous caffeine is known to occur in two different polymorphic phases (called I and II), which constitute an enantiotropic system.¹ The commercial form (II) is thermodynamically stable at room temperature and transforms upon heating at about 426 K^2 into form I which is characterized as a disordered crystalline state from calorimetric and X-ray investigations.³ This state can be maintained at low-temperature in a very slowly relaxing metastable situation. The I→II transformation is hindered at room temperature⁴ but kinetics of transformation are significantly faster around 363 K . Dielectric⁵ and X-ray³ investigations in the undercooled form I have revealed that this metastable form is a dynamically and orientationally disordered state, i.e., a rotator phase also called plastic crystal. Time-resolved dielectric investigations of relaxation kinetics in the metastable form I,⁶ and in the different polymorphic forms by the technique of thermally stimulated depolarization currents⁷ (TSDC) also suggest the existence of a dynamical disorder in the stable form II. Indeed, TSDC results⁷ can be interpreted (i) from consideration that the molecular mobility in form II is identical to that observed in form I, with similar activation parameters and identical distribution of relaxation times or (ii) by considering a significant amount of form I ($\sim 25\%$) coexisting with form II. A detailed computational study⁸ shows an orthorhombic crystal structure of form II, characterized by antiparallel-stacked dimers. Recent

X-ray diffraction experiments converge into a structural organization of molecules in an intriguing large monoclinic cell^{9,10} suggesting that the existence of disorder should be considered to obtain a correct structural description of the stable form. In addition, consideration of such a large unit cell suggests necessarily the presence of many Bragg peaks in the 2θ range $2\text{--}10^\circ$ using $\text{CuK}\alpha_1$ radiation, while no peak can be detected below 15° in the diffraction pattern of form II.¹⁰ Consequently, the organization and the dynamics of caffeine molecules in the stable crystalline form can be considered as being only roughly described. Obtaining pure crystallographic phases and predicting polymorph stability can be considered as the archetype of pharmaceutical challenges in solid-state drug processing. In this context, precise information on the molecular disorder and the structural organization in form II is required for a better description of the polymorphism in caffeine.

Raman spectroscopy is an indirect structural probe of the long-range order^{11,12} through the analysis of the phonon peaks in the low-frequency range, and also of the close molecular neighboring via the analysis of intramolecular vibrations in the high frequency range.¹³ Raman spectroscopy is also very sensitive to orientational disorder in rotator phases,^{14–16} by contrast to X-ray

Received: December 20, 2010

Revised: March 14, 2011

Published: April 22, 2011

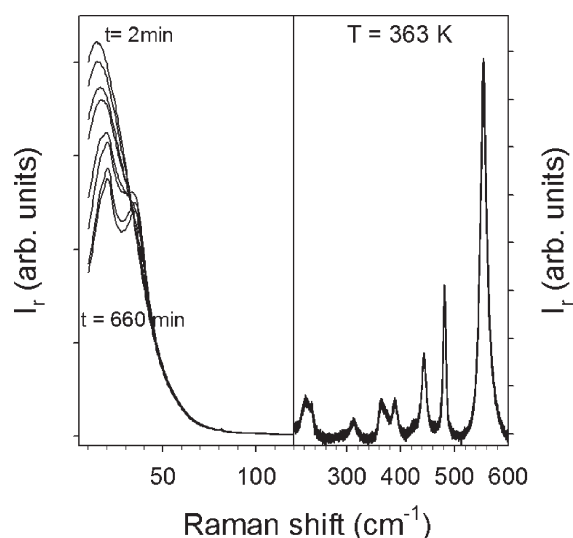


Figure 1. Time dependence of the reduced intensity in the 10–600 cm^{-1} range.

diffraction, since Bragg peaks reflect the periodicity of the mass centers of molecules.

In a first step, the purified sample, in metastable form I, was heated at 363 K to analyze the isothermal I \rightarrow II transformation in the 10–600 cm^{-1} low-frequency range (LFRS). After transformation, the temperature dependence of the LFRS was analyzed in the domain of stability of form II between 90 and 426 K. Upon further heating, form I was obtained, and in a second step, the LFRS of form I was analyzed in the 90–513 K range, and in the liquid state up to 543 K. The Raman spectra of the different states of caffeine, i.e., the liquid state and crystalline forms I and II, were compared.

In order to obtain a better insight on the nature of form II of caffeine, the LFRS of theophylline was compared to that of form II of caffeine. Theophylline ($\text{C}_7\text{H}_8\text{N}_4\text{O}_2$) and caffeine have a similar molecular structure, based on the parent purine ring skeleton, in which two of the four nitrogen atoms in theophylline are methylated, instead of three in caffeine. The packing arrangement in anhydrous theophylline described in an orthorhombic cell ($Pna2_1$, $Z = 4$) from different experimental investigations and lattice energy calculations,¹⁷ can be considered as not so far from that of form II of caffeine,^{9,10} with the exception that theophylline molecules are located on ordered sites and form a bilayer structure via N–H \cdots N and C–H \cdots O hydrogen bonding not existing in caffeine.

II. EXPERIMENTAL METHODS

Caffeine. Caffeine (98.5% purity) was purchased from Acros Organics and was purified by cold sublimation: caffeine was sublimated at 493 K and 10^{-3} Torr onto a coldfinger (at 12 $^{\circ}\text{C}$). Pure form I is obtained by heating purified caffeine above the II \rightarrow I transition temperature (426 K).

Theophylline. Theophylline (99% purity) was obtained from Acros Organics and used as supplied.

Raman Spectroscopy. Raman spectra were recorded in the 10–600 cm^{-1} range, in VV+VH geometry, to obtain a non-polarized light-scattering spectrum under a scattering angle $\theta = 180^{\circ}$, using the 514.5 nm line of a mixed argon–krypton Coherent laser. The Dilor spectrometer is composed of a double monochromator comprising four mirrors characterized by a focal

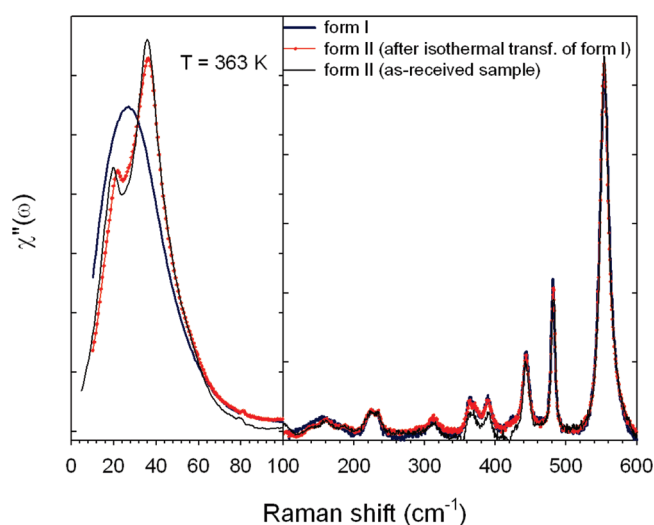


Figure 2. Raman susceptibility in the crystalline forms I and II in the 10–600 cm^{-1} frequency range. Form II can be represented by the spectrum recorded at the end of the isothermal transformation, and by the spectrum of the as-received sample without purification heated at 363 K.

length of 800 mm, and a spectrograph. The entrance and exit slits are opened and kept to 200 μm , determining the incident radiation resolution of nearly 2 cm^{-1} in the investigated frequency range. The spectrometer is equipped with a liquid nitrogen-cooled charge coupled device detector. The high sensitivity of the detector and the large analyzed scattered volume ($\sim 0.4 \text{ cm}^3$) allowed us to record Raman spectra in the 10–600 cm^{-1} range in 2 min, without moving the monochromator and spectrograph. Caffeine powder ($\sim 0.4 \text{ cm}^3$) was loaded in a spherical pyrex cell hermetically sealed. The temperature of the sample was regulated using an Oxford nitrogen-flux device that keeps temperature fluctuations within 0.1 $^{\circ}\text{C}$.

III. RESULTS

III.1. Isothermal Transformation of the Raman Spectrum in the 10–600 cm^{-1} Region. The purified sample which is in the metastable form I, was first heated in the temperature domain of faster transformation (363 K), and maintained at this temperature for the analysis of the isothermal dependence of the Raman spectrum in the low-frequency range (10–600 cm^{-1}). The spectra were recorded by steps of 5 min, and are plotted in Figure 1 by steps of 60 min. In order to avoid the distortion of the low-frequency Raman band shape^{18–20} induced by temperature fluctuations, the Raman intensity $I(\omega)$ was converted into the reduced intensity $I_r(\omega)$ according to $I_r(\omega) = I(\omega)/([n(\omega) + 1]\omega)$, where $n(\omega) = [\exp(\hbar\omega/k_B T) - 1]^{-1}$ is the Bose–Einstein occupation number with k_B being the Boltzmann constant. Two spectral regions, characterized by different time dependences, can be distinguished. The low-frequency Raman spectrum lying from 10 to 100 cm^{-1} , exhibits significant changes between $t = 0$ and $t \approx 9 \text{ h}$, while above 100 cm^{-1} the spectra are rigorously superimposed. No significant change of the Raman spectrum in the 10–100 cm^{-1} range can be detected after about 9 h, and then recording spectra was stopped after about 32 h of isothermal aging.

In molecular crystals, the intramolecular bonding is very strong compared with the weak intermolecular bonding. Consequently,

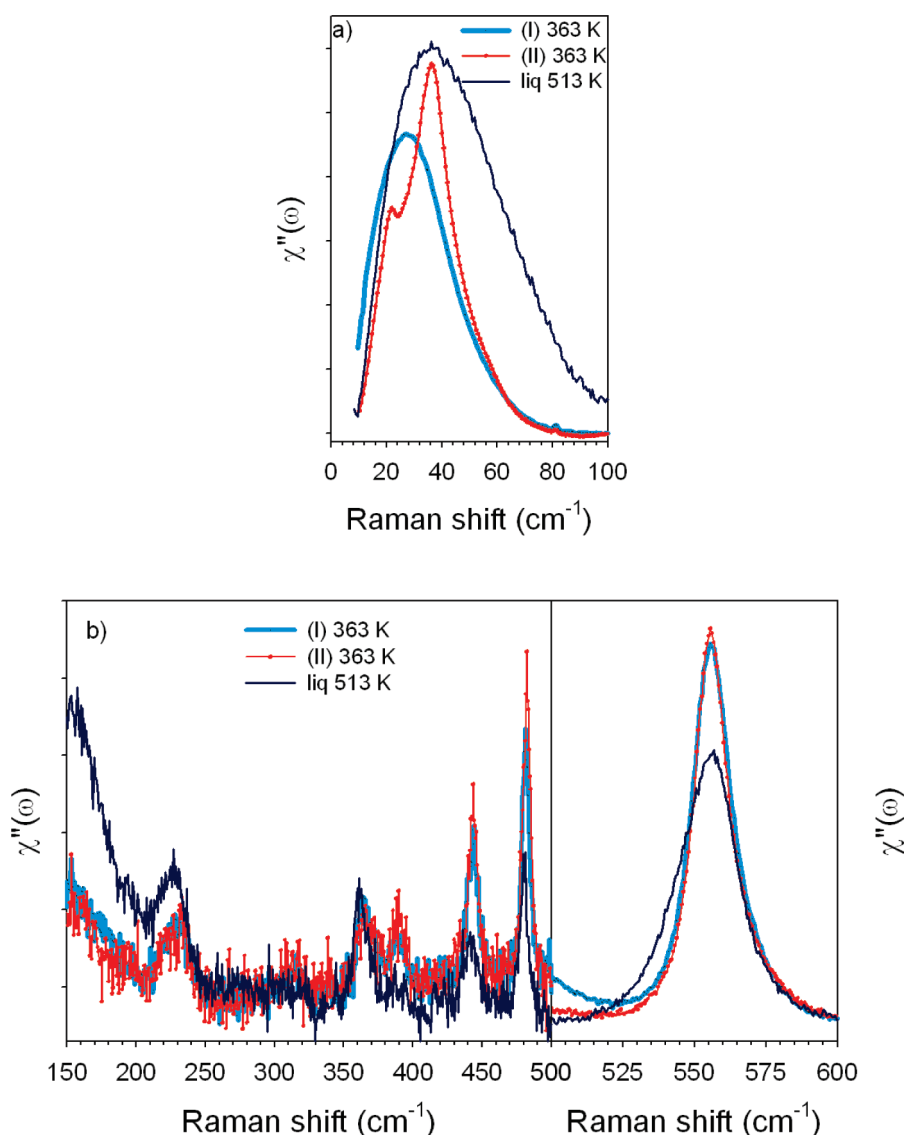


Figure 3. Representation of Raman susceptibility in the 10–600 cm^{-1} frequency range in forms I and II at 363 K, and in the liquid state at 513 K (a) for collective motions in the 10–100 cm^{-1} range and (b) for an internal vibrational bands the 150–600 cm^{-1} range.

there is a disparity between force constants in molecular solids,²¹ which is reflected in the Raman spectra by a spectral gap between external and internal peaks. In this context, it can be considered as a general property of the molecular compounds that external and internal motions can be treated as separable,²² and hence imply that the molecule moves under the influence of the lattice modes as a rigid body.²² For caffeine, internal modes are detected above 100 cm^{-1} . The Raman band shape of internal modes is highly dependent on the close molecular neighboring and the absence of spectral modification in the 100–600 cm^{-1} frequency range during the transformation, and indicates a similar local order in the two crystalline forms. The low-frequency Raman spectrum of phase I of caffeine (below 100 cm^{-1}) is dominated by a very broad band distinctive of a highly disordered system.^{14,19,20} In disordered molecular compounds, the low-frequency intensity results from the overlapping contributions of semiexternal or semi-internal motions and external motions. The first contribution corresponding to the quasielastic intensity is associated with large amplitude motions of the molecule or a

group of atoms within the molecule, while the latter corresponds to intermolecular or collective motions. After subtracting the quasielastic component determined from a fitting procedure widely detailed for several molecular compounds,^{12,20} the reduced intensity was converted into Raman susceptibility using the relation $\chi''(\omega) = \omega \cdot I_r(\omega)$. It is plotted in Figure 2, for the metastable state of form I at the beginning of the isothermal transformation ($t = 0$) at 363 K, and in a state close to form II after about 32 h of isothermal transformation. These spectra are compared to that of the as-received sample at 363 K, considered as mostly in form II.

As expected, from the broad band shape of the low-frequency spectrum plotted in Figure 1, no phonon peak can be distinguished in the Raman susceptibility of the phase (I). Such a band shape for the low-frequency spectrum reflects a high degree of disorder, as observed in the crystalline rotator phase characterized by a high orientational disorder,^{14,15,23} in agreement with previous investigations suggesting the existence of a dynamical orientational disorder in phase I.⁵ In amorphous states, the Raman susceptibility can be related to the vibrational density

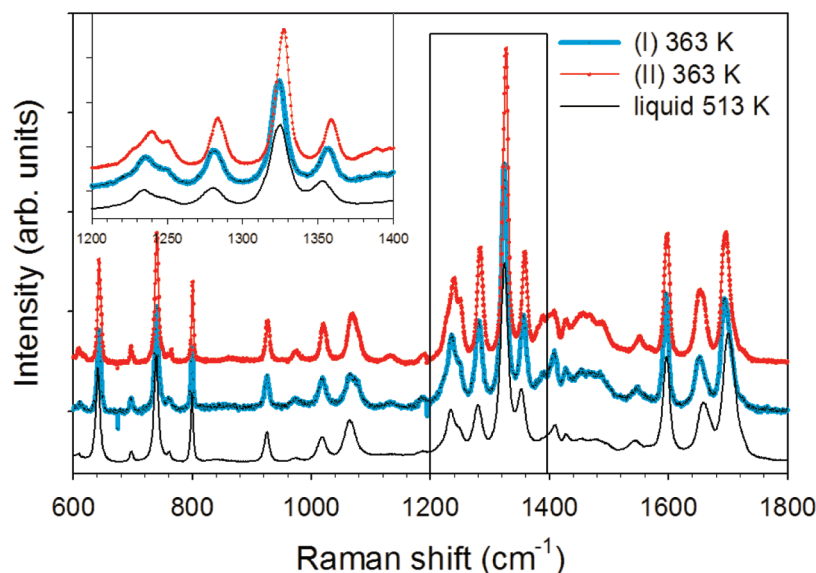


Figure 4. The Raman intensity in the 600–1800 cm^{-1} frequency range in the crystalline forms I and II at 363 K and in the liquid state at 513 K. The inset corresponds to the 1200–1400 cm^{-1} region to clearly show the slight frequency shift of the most intense band after isothermal transformation of phase I into phase II.

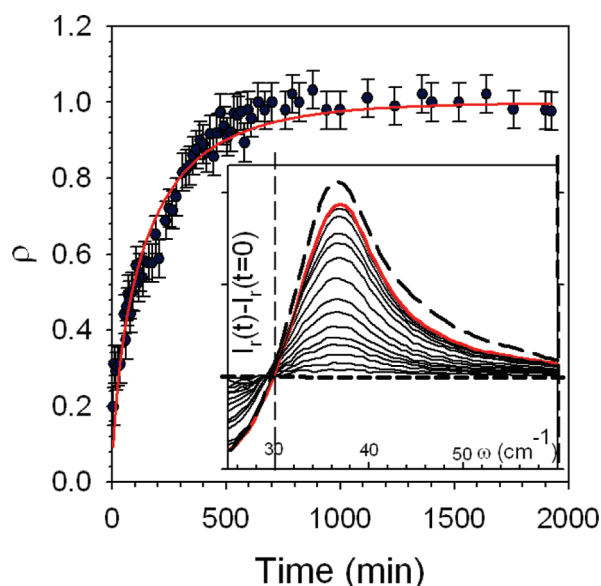


Figure 5. Kinetics law obtained from the analysis of the low-frequency reduced intensity. The line corresponds to the fitting procedure described in the text. The spectrum difference $[I_r(t) - I_r(t=0)]$ used to calculate $\rho(t)$ is plotted in the inset between 25 and 60 cm^{-1} , from $t = 5$ min in increments of 30 min. The dashed line in the inset corresponds to the spectrum difference at 363 K between the as-received sample and form I at the beginning of the isothermal transformation.

of states $G(\omega)$, according to^{24,25} $\chi''(\omega) = \omega \cdot I_r(\omega) = G(\omega) \cdot C(\omega)/\omega$, where $C(\omega)$ is the light-vibration coupling coefficient. In contrast to amorphous states, rotator phases have a periodic lattice generated by the mass centers of molecules, and then can be rigorously considered as crystalline phases characterized by a space group. It was shown that the low-frequency Raman spectrum of a rotator phase is dominated by librational motions.^{16,23,26} The clear amorphous-like band-shape of the low-frequency Raman spectrum

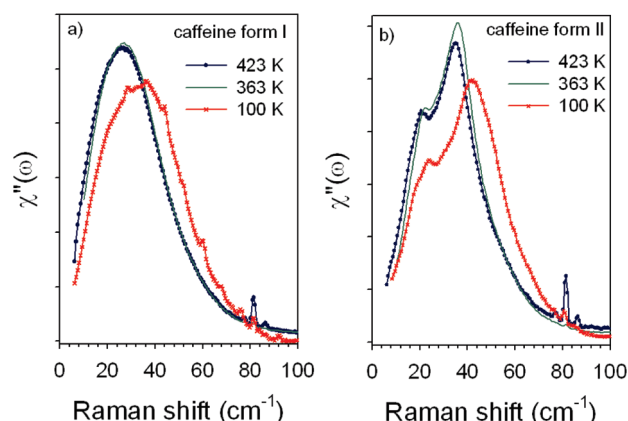


Figure 6. Temperature dependence of the Raman susceptibility corresponding to the density of librational states in form I (a) and in form II (b).

in rotator phases corresponds to the envelope of librational frequencies experienced by a central molecule located in different molecular environments. In this context, the Raman susceptibility in orientationally disordered phases is related to the librational density of states $G_L(\omega)$, according to the relation²³ $\chi''(\omega) = [C(\omega)/\nu]G_L(\omega)$. It is worth noting that the physical state of form I is really crystalline despite the amorphous-like band-shape of the LFRS, contrasting with the observation of sharp Bragg peaks in the X-ray diffraction pattern.³

The Raman susceptibility in phase II is easily distinguishable from that of form I. It is dominated by a double hump that appears as a splitting of the broad band observed in the spectrum of phase (I). The two low-frequency components emerging during the isothermal transformation are too broad to be considered as two phonon peaks, reflecting a significant degree of disorder. It is observed in Figure 2, that the spectrum of the as-received sample is slightly different from that recorded after 32 h of isothermal aging. The splitting of the low-frequency bands is

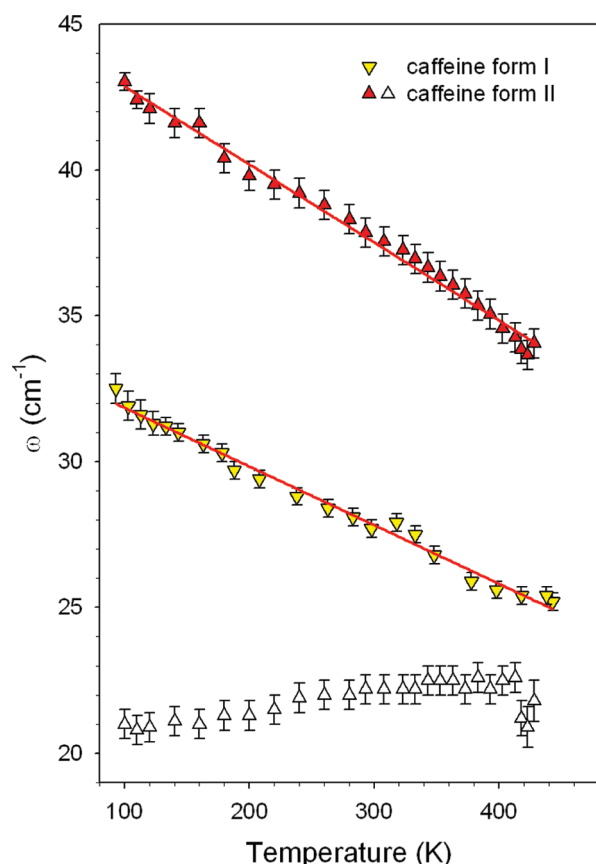


Figure 7. $\omega(T)$ curves of the low-frequency bands in forms I and II; the lines correspond to linear regressions.

more marked in the spectrum of the as-received sample than in that recorded after 32 h of isothermal transformation. Consequently, the differences between the two spectra suggest the existence of a residual amount of form I coexisting with form II.

Phase (I) of caffeine was also heated up to 523 K to record the Raman spectrum of the liquid state. The $\chi''(\omega)$ spectra taken in form I and II at 363 K and in liquid state at 523 K are plotted in Figure 3a for the low-frequency range (below 100 cm^{-1}) and in Figure 3b for the internal vibrational bands below 600 cm^{-1} . Above the melting temperature ($T_m = 509$ K), the Raman susceptibility broadens and shifts toward the high frequencies. In the liquid state, the broad band reflects molecular motions restricted by the close molecular neighboring. The broadening of the Raman susceptibility in the liquid state results from the contribution of the different kinds of collective motions (librations + vibrations), while the Raman susceptibility in the rotator crystalline phases is mainly dominated by librational motions. Figure 3b shows that the shape of the 555 cm^{-1} band, assigned to the CNC and O=CN deformations²⁷ in the pyrimidine ring, is significantly broadened in the liquid state.

The Raman spectrum in the 600–1800 cm^{-1} region plotted in Figure 4, corresponds to the fingerprint region of a molecular compound, since it is composed of intramolecular vibrations distinctive of the atomic bonds, the molecular conformations, and the close molecular neighboring. This spectral region is plotted for the liquid state and both crystalline forms. In contrast to the 10–100 cm^{-1} low-frequency range, the analysis of the 600–1800 cm^{-1} region indicates that the local order is very

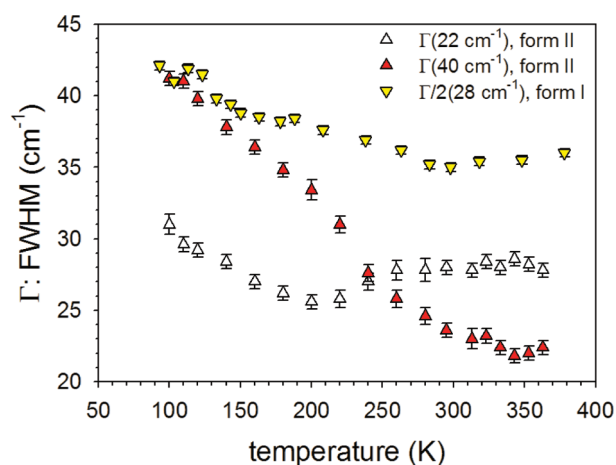


Figure 8. $\Gamma(T)$ curves corresponding to the temperature dependence of the full width at half maximum (fwhm) of the low-frequency bands in forms I and II. In form I, the half width ($\Gamma/2$) is plotted, to give a clear comparison with the band widths in form II on the same scale.

similar in the three states, indicating the existence of disordered molecular environments in both crystalline forms, in agreement with spectra recorded in the 100–600 cm^{-1} range. The Raman spectra of the liquid state and form I can not be distinguished above 100 cm^{-1} , confirming that the dynamically orientationally disordered state of rotator phases represents the true analogue of a supercooled liquid.²⁸ Only slight frequency shifts of some internal modes can be detected in the spectrum of phase II, as shown in the inset of Figure 4 for the most intense band of the spectrum corresponding to the imidazole ring stretching vibration.²⁹ No trace of ordering is really detected in the Raman spectrum of form II above 100 cm^{-1} , confirming the existence of an orientational disorder suggested from previous experiments.^{6,7,9,10}

III.2. Analysis of the Transformation Kinetics. In previous works,^{12,30} it was shown that the integrated intensity of low-frequency Raman signatures of a growing phase could be related to a degree of transformation. The reduced intensity was integrated between 30 and 60 cm^{-1} , where a shoulder is observed to grow during the isothermal transformation I \rightarrow II. The degree of this transformation is determined from the relation $\rho(t) = [\int_{30}^{60 \text{ cm}^{-1}} I_r(t) - I_r(t=0)] / [\int_{30}^{60 \text{ cm}^{-1}} I_r(t_{\text{end}}) - I_r(t=0)]$, where t_{end} is chosen as $t \approx 1900$ min. The time dependence of this degree of transformation is reported in Figure 5. It is worth noting that the spectrum recorded at $t \approx 1900$ min does not rigorously correspond to the spectrum of form II. The inset of Figure 5 shows that the spectrum difference $[I_r - I_r(t=0)]$ between the reduced intensities of the as-received sample (I_r) and the first spectrum recorded at the beginning of the transformation ($I_r(t=0)$) plotted as a dashed thick line, is clearly different from the $I_r(t_{\text{end}}) - I_r(t=0)$ plotted as a solid thick line. This indicates that form I is not totally transformed into form II. It can be estimated that after 1900 min, about 93% of the sample is transformed into form II, using $\rho(t)$ -calculation with $\rho = 1$ for the as-received sample. Figure 5 reveals that the kinetics is very fast at the earliest stage of transformation, while it becomes very slow at longer times. The time evolution of $\rho(t)$ can be fitted using the function $\rho(t) = 1 - \exp[-(t/\tau)^n]$ and only by considering $\rho = 1$ at $t \approx 1900$ min. The fitting procedure gives an exponent $n = 0.69 \pm 0.03$ and $\tau = 147.7 \pm 5.5$ with a coefficient determination $R^2 = 0.956$. Such an exponent value close to 0.7 is associated with an unusual stretched exponential law for the nucleation and growth process, which is

Table 1. Slopes of $\omega(T)$ Curves Determined by a Linear Regression in the Two Forms of Caffeine for the Low-Frequency Bands (Located around 28 cm^{-1} in Form I, and 38 cm^{-1} in Form II) and for the 555 cm^{-1} Band

	low-frequency bands $\partial\omega/\partial T$ (cm^{-1}/K)	555 cm^{-1} band $\partial\omega/\partial T$ (cm^{-1}/K)
form I	$-2.1 \times 10^{-2} (\pm 5.10^{-4})$	$-6.4 \times 10^{-3} (\pm 10^{-4})$
form II	$-2.7 \times 10^{-2} (\pm 5.10^{-4})$	$-6.5 \times 10^{-3} (\pm 10^{-4})$

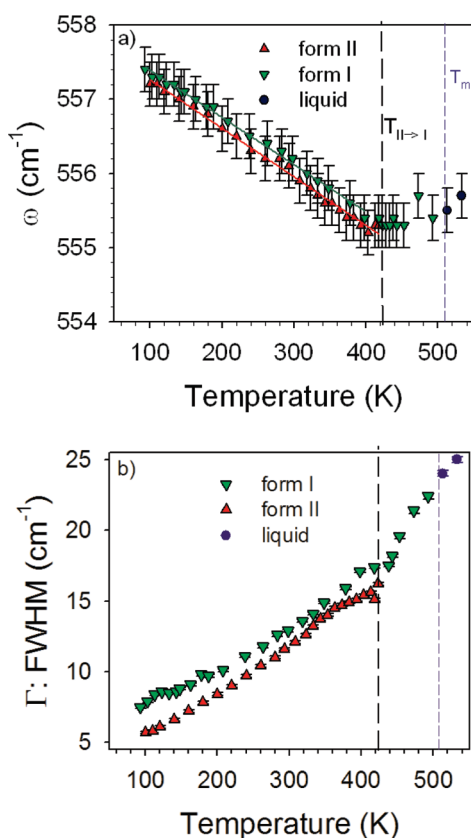


Figure 9. Temperature dependence of the 555 cm^{-1} band in forms I and II and in the liquid state: (a) $\omega(T)$ curves; (b) $\Gamma(T)$ curves. The vertical long-dashed line localizes the temperature of transformation of form II into form I, and the vertical short-dashed line indicates the melting temperature.

generally characterized by a sigmoidal shape. The kinetics law is similar to that obtained from different kinds of experiments,^{4,6,31} and has been interpreted from the consideration that the isothermal transformation is driven by nucleation with the maximum rate at higher temperature⁶ in crystallites characterized by a wide size distribution, in agreement with observations performed using an atomic force microscope.³¹ The kinetics of transformation $\text{I} \rightarrow \text{II}$ was recently interpreted on the basis of a penetration model³¹ in which it was considered that form II propagated inward from the crystallite surface.

III.3. Temperature Dependence of the LFRS of Forms I and II. The Raman spectra of forms I and II were recorded in the $5\text{--}600\text{ cm}^{-1}$ range in the $90\text{--}420\text{ K}$ temperature range, and are plotted in Figure 6 at three temperatures. The immediate consequence of such a comparison regards the existence of a significant disorder in form II as demonstrated by the absence of

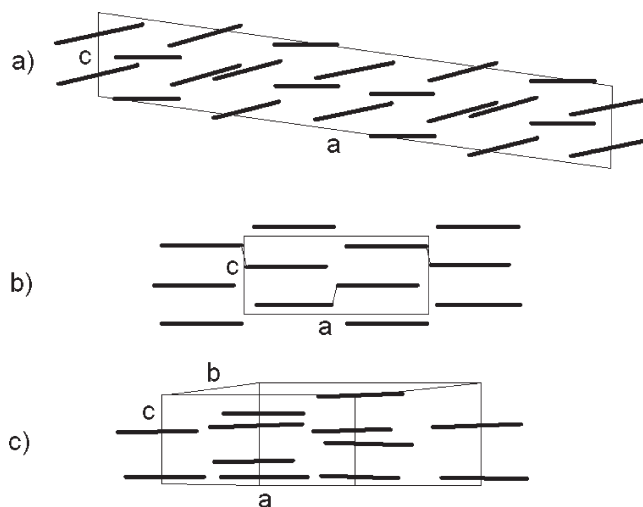


Figure 10. Representation of the molecular packing of caffeine in the (a, c) plane (a) in form II according to Enright et al.,⁹ (b) in form II according to Carlucci and Gavezotti,⁸ and (c) in form I according to Derollez et al.³

well-resolved phonon peaks even at low-temperature. Moreover, Figure 6 clearly shows that the Raman bands broaden upon cooling in both forms, whereas the opposite behavior is usually observed in ordered crystalline phases. It can also be observed that the low-frequency band in form II is nearly temperature independent, contrasting the behavior of the high-frequency band. The frequencies and widths of the Raman bands in the spectra of the two crystalline forms were determined from fitting procedures using log-normal distribution, which was determined to be very suitable to describe the Raman band shapes,^{32,33} and their temperature dependences are plotted in Figure 7 and 8. It is confirmed that the band detected at 22 cm^{-1} in form II does not shift significantly, while the frequency of the second band exhibits a temperature behavior similar to that of the broad band in form I. The experimental $\omega(T)$ curves were analyzed using a linear regression, and the corresponding slopes are reported in Table 1, except for the 22 cm^{-1} band in the spectrum of form II, which is nearly temperature independent in the $90\text{--}426\text{ K}$ temperature range. Interestingly, it is observed in Figure 8 that the width of the Raman bands (in the two forms of caffeine) increases upon cooling below room temperature, especially that located around 40 cm^{-1} in form II. This inhomogeneous broadening reflects a more heterogeneous distribution of molecular orientations at low temperature associated with a strong static (orientational) disorder. The temperature dependence of the frequency and the width of the 555 cm^{-1} band were analyzed and plotted in Figure 9a,b, respectively. A change in the slopes of $\omega(T)$ and $\Gamma(T)$ is clearly observed near 420 K , i.e., around the temperature of transformation ($T_{\text{II} \rightarrow \text{I}}$) of form II toward form I, while no signature of the melting temperature can be detected in the temperature behavior of this band. The slopes of $\omega(T)$ curves are determined and reported in Table 1. $\partial\omega/\partial T$ values are very similar for both forms and significantly lower than those determined for the broad low-frequency bands, as expected for internal motions. The frequency becomes temperature independent above 420 K , indicating that the close molecular neighboring has no influence on the internal vibrations corresponding to CNC and O=CN deformations in the pyrimidine ring. The strong and monotonic broadening of this band above 420 K

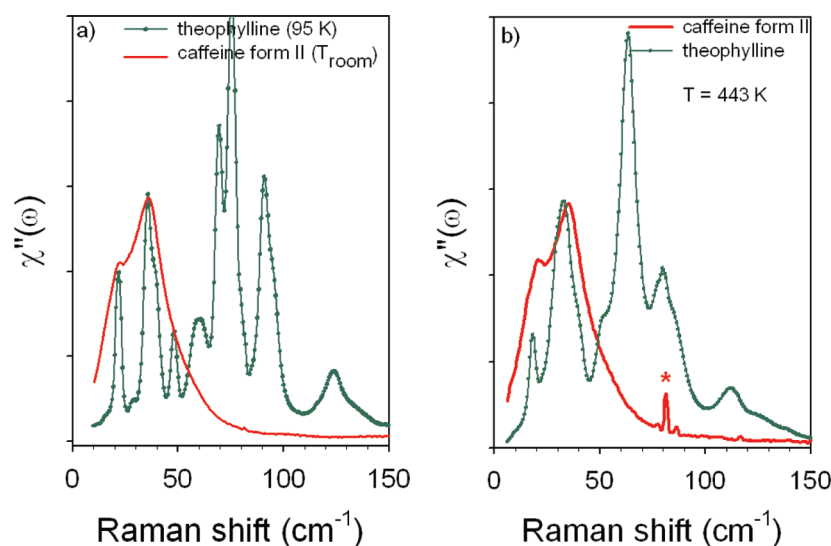


Figure 11. Comparison between Raman susceptibilities of form II of caffeine and theophylline in the low-frequency range: (a) the Raman spectrum of caffeine at room temperature is compared with that of theophylline at low-temperature; (b) the two spectra are compared at high temperature $T = 443$ K. The star indicates a laser line.

indicates that the 555 cm^{-1} band is very sensitive to the rotational disorder, and this disorder is similar in form I and the liquid state of caffeine. Below 420 K , the $\Gamma(T)$ curve in the metastable form I becomes similar to that in form II reflecting a similar progressive freezing of the rotational molecular motions in both crystalline forms. In a low-temperature regime, $\Gamma(T)$ in form I deviates from that in form II, suggesting the persistence of the rotational disorder in form I at low-temperature.

IV. DISCUSSION

Both low and high frequency investigations are converging into a description of form II as a disordered phase.

In the low-frequency range ($5\text{--}100\text{ cm}^{-1}$), the isothermal $\text{I} \rightarrow \text{II}$ transformation is characterized by the splitting of the band reflecting the density of librational states in form I into two components. This can be interpreted as corresponding to two different frequency distributions of rotational motions, which could be related to two different tilts of the molecular plane out of the (a,b) plane, as shown in Figure 10. It is worth noting that the two low-frequency bands are too broad to be considered as phonon peaks, and their broadening upon cooling could be associated with the existence of different tilts of the molecules, as predicted from X-ray investigations.^{9,10} Bragg peaks mainly reflect the periodicity of mass centers of molecules, but do not provide specific information about their orientation. However, the reduction of the intensity of Bragg peaks as 2θ increases, observed in the diffraction pattern of form II,¹⁰ suggests large Debye–Waller factors distinctive of dynamical and orientational disorder. To give a better insight of the disorder in form II of caffeine, its low-frequency Raman spectra recorded at room temperature and 443 K are compared in Figures 11a and 11b with those of anhydrous theophylline at low temperature and 443 K . Figure 11a reveals that the spectrum of form II of caffeine at room temperature is the rigorous envelope of the sharp low-frequency phonon peaks of theophylline at low temperature in the very low-frequency range ($5\text{--}60\text{ cm}^{-1}$). This demonstrates that form II of caffeine can be described from the crystal packing

of theophylline at low-temperature and a contribution of dynamical disorder. Additional phonon peaks are detected in the spectrum of theophylline above 60 cm^{-1} , confirming that the spectra of forms I and II of caffeine are dominated by the contributions of rotational motions. It is clearly observed that the low-frequency phonons in theophylline broaden upon heating, as expected for quasi harmonic motions, while the widths of the broad bands in form II of caffeine remain nearly constant, reflecting a similar distribution of librational frequencies and then a similar local molecular environment at high temperature.

Investigations in the high frequency range (above 100 cm^{-1}) indicate a similar description of the local order and the dynamical disorder in form I and the liquid state. Figure 4 shows similar Raman spectra in the fingerprint region for the liquid state and forms I and II. Only a very slight frequency shift (weaker than 1 cm^{-1}) of the 1328 cm^{-1} can be detected. This band was assigned to CN stretching vibrations in the imidazole ring,²⁷ and can be considered as corresponding to the most sensitive internal mode to discriminate the highly disordered states (liquid state and crystalline form I) from the stable form II, probably because these vibrations are correlated to the tilt of molecules. This comparison confirms the existence of a strong orientational disorder in form II, characterized by a local order similar to that of form I or the liquid state. The similarities between the $\omega(T)$ and $\Gamma(T)$ curves in form II and metastable form I confirm the existence of orientational and dynamical disorder in form II, with a weaker rotation amplitude than in form I since the bands are systematically sharper in form II than in form I. In contrast to the low-frequency bands, the 555 cm^{-1} band exhibits a significant sharpening by lowering the temperature, probably reflecting the progressive freezing of the rotational motions. The monotonic sharpening of this band in form II observed by lowering the temperature can be correlated with the inhomogeneous broadening of the 40 cm^{-1} band, suggesting that the freezing of molecular rotations generates more disordered orientational positions.

From low- and high-frequency investigations, it can be considered that the dynamic disorder in form II is very similar to that in form I with restricted molecular rotations probably

imposed by the orientational positions occupied by molecules in form II.

V. CONCLUSION

The present Raman spectroscopy investigations reveal very close description of the local order and the rotational disorder in form I and the liquid state. Major Raman signatures of the isothermal transformation of the rotator phase (form I) into form II at 363 K are only detected in the low-frequency range, indicating a local order in form II similar to that in form I and in the liquid state. Both kinds of information obtained from low- and high-frequency analyses are converging into a description of form II as a rotator phase, in agreement with previous investigations.^{5,7} The close relationship between the low-frequency spectra of theophylline and form II of caffeine shows that the structural description of the latter can be given from the molecular packing arrangement similar to that of theophylline¹⁷ with a contribution of a dynamic reorientational disorder existing in form I. The present investigations combining low- and high-frequency analyses show that Raman spectroscopy is very suitable for the structural description of disordered states, since X-ray diffraction experiments^{9,10} have not evidenced dynamical disorder in form II.

REFERENCES

- (1) Bothe, H.; Cammenga, H. K. *J. Therm. Anal.* **1979**, *16*, 267.
- (2) Cesaro, A.; Starec, G. *J. Phys. Chem.* **1980**, *84*, 1345.
- (3) Derollez, P.; Correia, N.; Danede, F.; Affouard, F.; Lefebvre, J.; Descamps, M. *Acta Crystallogr.* **2005**, *B61*, 329.
- (4) Lehto, V. P.; Laine, E. *Thermocim. Acta* **1998**, *317*, 47.
- (5) Descamps, M.; Correia, N.; Derollez, P.; Danede, F.; Capet, F. *J. Phys. Chem. B* **2005**, *109*, 16092.
- (6) Decroix, A.-A.; Carpentier, L.; Descamps, M. *Philos. Mag.* **2008**, *88*, 3925.
- (7) Moura Ramos, J.; Correia, N.; Diogo, H.; Descamps, M. *J. Phys. Chem. B* **2006**, *110*, 8268.
- (8) Carlucci, L.; Gavezzotti, A. *Chem.—Eur. J.* **2005**, *11*, 271.
- (9) Enright, G.; Terskikh, V.; Brouwer, D.; Ripmeester Cryst. Growth Des. **2007**, *7*, 1406.
- (10) Lehmann, C.; Stowasser, F. *Chem.—Eur. J.* **2007**, *13*, 2908.
- (11) Hedoux, A.; Guinet, Y.; Descamps, M. *Phys. Rev. B* **1998**, *58*, 31.
- (12) Hédoux, A.; Paccou, L.; Guinet, Y.; Willart, J.-F.; Descamps, M. *Eur. J. Pharm. Sci.* **2009**, *38*, 156.
- (13) Hedoux, A.; Hernandez, O.; Lefebvre, J.; Guinet, Y.; Descamps, M. *Phys. Rev. B* **1999**, *60*, 9390.
- (14) Denicourt, T.; Hedoux, A.; Guinet, Y.; Willart, J. F.; Descamps, M. *J. Phys. Chem. B* **2003**, *107*, 8629.
- (15) Affouard, F.; Hédoux, A.; Guinet, Y.; Denicourt, T.; Descamps, M. *J. Phys.: Condens. Matter* **2001**, *13*, 355011.
- (16) Guinet, Y.; Sauvajol, J.-L.; Muller, M. *Mol. Phys.* **1988**, *65*, 723.
- (17) Smith, E.; Hammonnd, R.; Jones, M.; Roberts, K.; Mitchell, J.; Price, S.; Harris, R.; Apperley, D.; Cherryman, J.; Docherty, R. *J. Phys. Chem. B* **2001**, *105*, 5818.
- (18) Achibat, T.; Boukenter, A.; Duval, E. *J. Chem. Phys.* **1993**, *99*, 2046.
- (19) Wypych, A.; Guinet, Y.; Hédoux, A. *Phys. Rev. B* **2007**, *76*, 144202.
- (20) Hédoux, A.; Guinet, Y.; Derollez, P.; Hernandez, O.; Paccou, L.; Descamps, M. *J. Non-Cryst. Sol.* **2006**, *352*, 4994.
- (21) Cochran, W.; Pawley, G. S. *Proc. R. Soc. A* **1964**, *280*, 1.
- (22) Venkataraman, G.; Sahni, V. C. *Rev. Mod. Phys.* **1970**, *42*, 409.
- (23) Rolland, J.-P.; Sauvajol, J.-L. *J. Phys. C: Solid State Phys.* **1986**, *19*, 3475.
- (24) Shuker, R.; Gammon, R. *Phys. Rev. Lett.* **1970**, *25*, 222.
- (25) Fontana, A.; Rossi, F.; Fabiani, E. *J. Non-Cryst. Sol.* **2006**, *352*, 4601.
- (26) Sauvajol, J.-L.; Bee, M.; Amoureux, J.-P. *Mol. Phys.* **1982**, *46*, 811.
- (27) Edwards, H. G. M.; Munshi, T.; Anstis, M. *Spectrochim. Acta, Part A* **2005**, *61*, 1453.
- (28) Brand, R.; Lunkenheimer, P.; Loidl, A. *J. Chem. Phys.* **2002**, *116*, 10386.
- (29) Pavel, I.; Szeghalmi, A.; Moigno, D.; Cinta, S.; Kiefer, W. *Biopolym. Biospectrosc. Sect.* **2003**, *72*, 25.
- (30) Hedoux, A.; Guinet, Y.; Descamps, M. *J. Raman Spectrosc.* **2001**, *32*, 677.
- (31) Kishi, Y.; Matsuoka, M. *Cryst. Growth Des.* **2010**, *10*, 2916.
- (32) Malinowski, V. K.; Novikov, V. N.; Sokolov, A. P. *Phys. Lett. A* **1991**, *153*, 63.
- (33) Hédoux, A.; Guinet, Y.; Derollez, P.; Hernandez, O.; Lefort, R.; Descamps, M. *Phys. Chem. Chem. Phys.* **2004**, *6*, 3192.